

Research Paper

Overexpression of Insulin-Like Growth Factor 1 Enhanced the Osteogenic Capability of Aging Bone Marrow Mesenchymal Stem Cells

Ching-Yun Chen^{1, 2}, Kuo-Yun Tseng³, Yen-Liang Lai^{2, 4}, Yo-Shen Chen^{1, 5}, Feng-Huei Lin^{1, 2}✉, Shankung Lin^{3, 6}✉

1. Institute of Biomedical Engineering, College of Medicine and College of Engineering, National Taiwan University, Taipei, Taiwan (R.O.C.);
2. Institute of Biomedical Engineering and Nanomedicine (I-BEN), National Health Research Institutes, Miaoli, Taiwan (R.O.C.);
3. Institute of Cellular and System Medicine, National Health Research Institutes, Miaoli, Taiwan (R.O.C.);
4. Ph.D. Program in Tissue Engineering and Regenerative Medicine, National Chung Hsing University, Taichung, Taiwan (R.O.C.);
5. Department of Plastic Surgery, Far Eastern Memorial Hospital, New Taipei City, Taiwan (R.O.C.);
6. Graduate Institute of Basic Medical Science, China Medical University, Taichung, Taiwan (R.O.C.).

✉ Corresponding authors: Shankung Lin, Assistant Investigator, Institute of Cellular and System Medicine, National Health Research Institutes, No. 35, Keyan Road, Zhunan Town, Miaoli 35053, Taiwan (R.O.C.). Tel: +886-37-246166 ext. 37302 Fax: +886-37-587409 E-mail: shankung@nhri.org.tw; Dr. F.H. Lin: double@ntu.edu.tw

© Ivyspring International Publisher. This is an open access article distributed under the terms of the Creative Commons Attribution (CC BY-NC) license (<https://creativecommons.org/licenses/by-nc/4.0/>). See <http://ivyspring.com/terms> for full terms and conditions.

Received: 2016.06.29; Accepted: 2016.12.08; Published: 2017.04.10

Abstract

Many studies have indicated that loss of the osteoblastogenic potential in bone marrow mesenchymal stem cells (bmMSCs) is the major component in the etiology of the aging-related bone deficit. But how the bmMSCs lose osteogenic capability in aging is unclear. Using 2-dimensional cultures, we examined the dose response of human bmMSCs, isolated from adult and aged donors, to exogenous insulin-like growth factor 1 (IGF-1), a growth factor regulating bone formation. The data showed that the mitogenic activity and the osteoblastogenic potential of bmMSCs in response to IGF-1 were impaired with aging, whereas higher doses of IGF-1 increased the proliferation rate and osteogenic potential of aging bmMSCs. Subsequently, we seeded IGF-1-overexpressing aging bmMSCs into calcium-alginate scaffolds and incubated in a bioreactor with constant perfusion for varying time periods to examine the effect of IGF-1 overexpression to the bone-forming capability of aging bmMSCs. We found that IGF-1 overexpression in aging bmMSCs facilitated the formation of cell clusters in scaffolds, increased the cell survival inside the cell clusters, induced the expression of osteoblast markers, and enhanced the biomineralization of cell clusters. These results indicated that IGF-1 overexpression enhanced cells' osteogenic capability. Thus, our data suggest that the aging-related loss of osteogenic potential in bmMSCs can be attributed in part to the impairment in bmMSCs' IGF-1 signaling, and support possible application of IGF-1-overexpressing autologous bmMSCs in repairing bone defect of the elderly and in producing bone graft materials for repairing large scale bone injury in the elderly.

Key words: IGF-1; bone marrow MSC; aging-related bone loss; osteoporosis; bioreactor.

Introduction

Instead of being a static organ, our skeleton constantly undergoes bone resorption and bone formation to replace old and damaged tissues as a part of bone remodeling process [1]. The balance between bone resorption and bone formation determines the outcome of bone remodeling [2]. It is

believed that the decrease in bone formation after each run of bone remodeling serves as a major cause of the age-related bone loss in men and women [3, 4]. The decrease of bone formation activity is also a major obstacle for the elderly to recover from large bone defect resulted from traumatic injury and surgery.

The findings that there are fewer osteoblasts in aging bones than in young bones [5-7], and that the impaired bone formation activity in aged humans can be attributed to insufficient osteoblasts [8-10] indicate an important role of mesenchymal stem cells (bmMSCs) in the etiology of aging-related bone deficit. It has been well established that bone marrow contains a small population of bmMSCs which are the precursor cells for many cell types, and among them is osteoblast, the workhorse in bone formation [11-16]. Examination of the cellular constituent in the regenerated marrows of adult and aged animals after marrow ablation revealed that bone marrows become more adipogenic than osteoblastogenic with aging [17, 18], indicating an alteration of lineage propensity of bmMSCs with aging. In fact, an increase in the commitment to adipogenic lineage and a decrease in the commitment to osteoblastic lineage have been found in the bmMSCs of aged mice [19]. These findings support the notion that the aging of bmMSCs, as manifested by the deficiency in the passage of bmMSCs to osteoblasts, accounts for the decrease of osteoblast production and the decline in bone formation activity with aging. Therefore, the improvement of osteogenic performance of aging bmMSCs could be a requisite step to boost bone formation in the elderly for the treatment of osteoporosis, and for possible application of autologous bmMSCs to repair bone defect of the elderly.

In addition to hormones, growth factors, especially the locally produced, function as mediators of skeletal growth and maintenance. Factors, such as platelet-derived growth factor (PDGF) [20, 21], fibroblast growth factor (FGF) [22, 23], and insulin-like growth factor 1 (IGF-1) [24, 25], act as bone cell mitogens [20-22]. IGF-1 also plays a central role in stimulating osteoblastic differentiation. A causative role that the compromised IGF-1 signaling plays in the aging-related decrease of bmMSCs' osteogenic capability and bone deficit is suggested by several informative findings [26, 27]. In experimental animals, it was found that the content of IGF-1 and the local expression of IGF-1 in bone decreased with aging [28-30]. It has also been shown that while IGF-1 could consistently activate genes that are related to osteogenic function, the mitogenic activity of IGF-1 was impaired in aged rats [24]. Notably, however, this defect could be corrected by higher dose of IGF-1 [24]. In experimental animals, direct infusion of IGF-1 into femur increased trabecular bone formation rate and trabecular bone mass in aged rats [31]. The information generated from murine systems inspire the idea that for possible application of autologous bmMSCs to repair bone defect of the elderly, a logical

approach is to increase IGF-1 production in the bmMSCs of aged patients. To support this, it will be important to determine whether the phenomena observed in murine systems also exists in human bmMSCs.

Recently, Chen et al. developed a bioreactor system for the production of bioactive bone graft materials from bmMSCs for clinical application [32]. In the system, cells were seeded into the intricate hydrogel-like structure of calcium-alginate scaffolds which provide cells a 3-dimensional environment mimicking the native microenvironment in a constantly perfused system for growing and osteogenic differentiation [32, 33]. This device could support human osteoblasts to proliferate and differentiate, and to form cell clusters. Such a device enabled us to quickly examine the bone-forming capability of bmMSCs receiving either genetic modulations or chemical treatments.

In this study, we examined the mitogenic activity of bmMSCs from adult and aged human donors in response to IGF-1. We also examined the effect of IGF-1 overexpression in the proliferation rate and osteoblastic potential of aging bmMSCs using conventional 2-dimensional cultures, and examined the effect of IGF-1 overexpression to the bone-forming capability of aging bmMSCs using the 3-dimensional bioreactor system.

Materials and Methods

Cell culture

Human bone marrow samples were collected from patients receiving total knee replacement surgery. Informed consent was obtained from each donor. The use of human bmMSCs in this study was approved by the Institutional Review Board of Miaoli General Hospital. Isolation of bmMSCs from marrow aspirates was performed as described previously [28]. Cells were cultured in Dulbecco's modified Eagle's medium (DMEM) (low glucose) (GIBCO-BRL) containing fetal bovine serum (15%) (Hyclone), glutamine, penicillin and streptomycin (GIBCO-BRL), and maintained in a humidified atmosphere containing 5% CO₂ at 37°C. Cell culture media were changed every 4 days. Cells cultured between the fourth and seventh passage were used in this study.

Plasmid construction

Human IGF-1 cDNA was amplified by PCR. The 5' and 3' primers used were: CACCATGGGTAAAATCAGCAGTCTTC; and CTACATCCTGTAGTTCTTGTTT. The cDNA was cloned into pLAS2w.Pneo vector (National RNAi Core Facility at Academia Sinica, Taiwan) to generate pLAS2w-IGF-1 for Lentivirus preparation.

Lentivirus preparation and infection

For IGF-1 overexpression in human bmMSCs, pLAS2w-IGF-1 was cotransfected with gag-pol and VSV-G-expressing plasmids into 293T cells. Viral supernatant was harvested 2 and 3 days after transfection and filtered through 0.45- μ m filters. For infection, bmMSCs were infected with virus (MOI = 40) for 3 h in the presence of polybrene (8 μ g/ml), and then maintained in regular medium.

Measurement of DNA synthesis

DNA synthesis was assessed by measuring the incorporation of 5-bromo-2-deoxyuridine (BrdU) into DNA using BrdU Cell Proliferation Assay kit based on the protocol provided by manufacturer (Millipore, MA, USA). Briefly, cells were treated with BrdU or phosphate buffer saline (as background control) for 24 h. Cells were then fixed and DNAs were denatured using the Fixing Solution. The BrdU label was detected by an anti-BrdU monoclonal antibody, and the signals were quantitated with a spectrophotometer microplate reader set at wavelength of 450/550 nm.

Induction of osteoblastic differentiation

For the induction of osteoblastic differentiation, confluent cultures were maintained in regular medium plus 0.1 μ M dexamethasone, 0.2 mM ascorbic acid 2-phosphate, and 10 mM glycerol 2-phosphate till the end of experiment, with medium changed every three days. At the end of experiments, cells were fixed and stained with 2% Alizarin Red S solution (Sigma-Aldrich, MO, USA) for 30 min at room temperature, and were de-stained with freshly prepared 10% Cetylpyridinium chloride (CPC) (Sigma-Aldrich, MO, USA) solution for 1 hour at room temperature with gentle rocking. The CPC solutions were then collected for the measurement of absorbance at 595 nm.

Quantitative real-time PCR (RT-qPCR)

Total RNA of cells culturing in 2-dimensional dishes was isolated using Trizol (Life Technologies, CA, USA). To isolate RNA from cells growing inside the calcium-alginate scaffolds, scaffolds were dissolved in 50 mM of EDTA solution, and the cells were collected by brief centrifugation. Total RNA was extracted using TriRNA pure kit (Geneaid). Total RNA was subjected to reverse transcription-PCRs to generate complimentary DNAs. RT-qPCR was performed using the Power SYBR Green PCR Master Mix (Applied Biosystems, CA, USA). The 5' and 3' primers used were as follows: IGF-1, TGCTCCGG AGCTGTGATCT and TCTGGGTCTTGGGCATGTC; Runx2, TTTGCACTGGGTTCATGTGTT and TGGCT

GCATTGAAAAGACTG; alkaline phosphatase, GACCCCTGACCCCCACAAT and GCTCGTACTG CATGTCCCCT; osteopontin, CTAGGCATCACCTG TGCCATACC and CAGTGACCAGTTCATCAGA TTCATC; IGF-1 receptor, TCGACATCCGCAA CGACTATC and CCAGGGCGTAGTTGTAGA AGAG; and β -actin, AAGTCCCTTGCCAT CCTAAAA and ATGCTATCACCTCCCCTGTG. RT-qPCRs were performed on an ABI PRISM 7000 Sequence Detector System. The relative mRNA levels were calculated using the $2^{-\Delta\Delta CT}$ method, with β -actin mRNA as a normalizer.

3-dimensional calcium-alginate scaffold fabrication

The calcium-alginate scaffolds were prepared as described previously [32, 33]. Briefly, 1.5 % sodium alginate (Keltone® LV) was poured into 48-well cell culture plates with the volume 1 ml/well. The plates were kept at -20°C overnight and then freeze-dried to allow the formation of porous structure. The highly porous scaffolds were cross-linked in 5% calcium chloride solution at room temperature for 1 h, and sterilized with 75% alcohol. The scaffolds were then freeze-dried once again, and stored at room temperature until use.

Continuous perfused bioreactor system

The continuous perfused bioreactor was constructed as described previously [32, 33]. Briefly, this bioreactor system comprises a 500 ml serum bottle as culture medium tank and a 50 ml conical sterile polypropylene centrifuge tube as cell culture tank. The scaffolds were placed in the cell culture tank. These two tanks were connected by tubing. The whole system were maintained in a humidified atmosphere containing 5% CO_2 at 37°C . The continuous medium supply was controlled via a peristaltic pump (LongerPump, China) with flow rate set at 1 ml/min.

Seeding human bmMSCs into calcium-alginate scaffolds

Human bmMSCs were suspended in culture medium and then seeded into calcium-alginate scaffolds (5×10^5 viable cells/scaffold) by injection. The scaffolds were placed in a non-coating 24-well culture plate and maintained for 24 h in a humidified atmosphere containing 5% CO_2 at 37°C , and then transferred into the dynamic perfused bioreactor system for 1, 7, 14, and 21 days.

Live/Dead staining

The cells-containing scaffolds retrieved from the bioreactor were stained for 30 min with 4 μ M of calcein AM (Life Technologies Inc., CA, USA) for live

cells, and with 4 μM of propidium iodide (PI, Life Technologies, Inc., USA) for dead cells. Live cells stained by calcein AM showed green fluorescence (ex/em $\sim 495\text{ nm}/\sim 515\text{ nm}$), whereas dead cells stained by PI showed red fluorescence (ex/em $\sim 540\text{ nm}/\sim 615\text{ nm}$). Cell survival rate was estimated by a confocal microscope (LSM 780, Zeiss, Germany), and the 3-dimensional images were reconstructed using the supplied software (ZEN lite, Zeiss, Germany).

Scanning electron microscopy (SEM) and size distribution analysis of human bmMSC clusters

The scaffolds with bmMSCs inside were fixed with 4% para-formaldehyde for 2 h, and dehydrated in a graded series of ethanol. The specimen was dried by critical-point drying (CPD) method, and were sputter-coated with gold before observation. The morphology of human bmMSC clusters was observed using SEM (TM-1000, Hitachi, Japan). For size distribution analysis of human bmMSC clusters, scaffolds were retrieved from the bioreactor at the time indicated. Then, bmMSC clusters were imaged by SEM. We measured the diameter of a round cell cluster and calculated the major axis of an elliptical one. The average diameters of the clusters were calculated with MetaMorph Microscopy Automation and Image Analysis Software (Molecular Devices, CA, USA). The definition of the diameter measurement was shown in supplemental Fig. S3. In addition, we investigated 20 to 35 cell clusters for each condition (Supplemental Fig. S4).

F-actin staining and predictive cell numbers of human bmMSC clusters

In order to estimate cell numbers of cell cluster, we also performed F-actin staining. Briefly, bmMSCs/scaffold constructs were fixed with 4% para-formaldehyde. The cell clusters were reacted with 1 drop ActinGreen 488 ReadyProbes Reagent (Life Technologies, Inc., USA) for 15 min, and counterstained with 1 $\mu\text{g}/\text{ml}$ Hoechst 33342 (Sigma-Aldrich, MO, USA) for 5 min, and observed by a confocal microscope (LSM 780, Zeiss, Germany). The data was analyzed by Imaris Scientific 3D/4D Image Processing & Analysis Software (Bitplane, CT, USA).

Xylenol orange staining

For the examination of biomineralization, scaffolds with bmMSCs inside were fixed with 4% para-formaldehyde. The cell clusters were rinsed with 20 μM xylenol orange (Sigma-Aldrich, MO, USA) for 15 min, and counterstained with 1 $\mu\text{g}/\text{ml}$ Hoechst 33342 (Sigma-Aldrich, MO, USA) for 5 min, and

observed by a confocal microscope (LSM 780, Zeiss, Germany). The biomineralized area of the cell clusters displayed the color of bright orange-red (ex/em $\sim 440\text{ nm}/\sim 610\text{ nm}$), whereas the nucleus displayed the color of blue. The 3-dimensional images were reconstructed using the supplied software (ZEN lite, Zeiss, Germany).

X-ray diffraction (XRD) and Fourier transform infrared spectroscopy (FT-IR)

XRD and FT-IR were used to identify crystal structure and functional groups of the deposit mineral, respectively, to conform that cells would secrete biological apatite. The deposit mineral was collected from the bioreactor and mounted to sample holder of XRD. XRD patterns were obtained by X-ray Powder Diffractometer (MiniFlex 600, Rigaku, Japan) under 20 Am and 15 eV; where 2θ would be recorded from 20° to 40° with scanning rate of $2^\circ/\text{min}$. The obtained patterns were compared to Crystallography Open Database (COD) for characterization.

The functional groups of the deposit mineral were analyzed by FT-IR spectroscopy (Spectrum 100 FT-IR Spectrometer, PerkinElmer, USA). The previously deposit mineral was added to the device of attenuated total reflection (ATR) for further analysis. The spectra and absorption bands were recorded in the wave number range of $4000\text{--}400\text{ cm}^{-1}$ with 16 scans per sample cycle. The absorption bands on the FT-IR spectrum were analyzed by Integrated Spectral Data Base System for Organic Compounds (SDBS).

Statistical analysis

Statistical difference was shown as the mean \pm standard deviation (S.D.) and conducted at least in triplicate. Student's t-test and one-way ANOVA followed by Scheffe's post hoc tests were used to analyze the data, and p -values less than 0.05 was considered statistically significant.

Results

Aging-related changes in the mitogenic response of human bmMSCs to IGF-1.

We analyzed the mitogenic response of bmMSCs derived from 4 adults (donor 1 to 4) and 10 aged (donor 5 to 14) human donors (Table 1) to various doses of IGF-1 by measuring the IGF-1-induced DNA synthesis using BrdU incorporation assays. The donor-specific data (raw data and donor-specific normalization data) were shown in the Supplemental Table S1. We analyzed the BrdU incorporation activity of adult and aged cells cultured without IGF-1 treatment (raw data), and found that there was no significant difference ($p = 0.420$) in the levels of DNA synthesis, as represented by OD₄₅₀ readings, between

the adult and aged cells (Fig. 1A). Due to the fact that one 96-well culture plate only allowed us to perform BrdU incorporation assay in cells from one donor, and that the OD₄₅₀ readings generated by cells either treated with various doses of IGF-1 or left untreated varied greatly among the cells (plates) regardless of the donor age, it was inadequate to do the inter-donor comparison based on the raw data. We, therefore, examined the effect of IGF-1 on the stimulation of DNA synthesis between donors based on the donor-specific normalization data. In adult group, significant increase in DNA synthesis was observed at IGF-1 dose of 5, 50, and 500 ng/ml, which induced approximately 63%, 64%, and 87% increase in DNA synthesis, respectively, whereas only 500 ng/ml of IGF-1 induced significant increase (~57%) in DNA synthesis in the aged group (Fig. 1B).

Table 1. Demography of bone marrow donors.

Donor	Gender	Age	Donor	Gender	Age
1	M	36	8	M	69
2	M	42	9	M	73
3	M	43	10	M	77
4	M	40	11	F	79
5	F	75	12	F	69
6	F	72	13	F	71
7	F	71	14	F	73

We calculated the fold-change in the stimulation of DNA synthesis in response to 5, 50, and 500 ng/ml of IGF-1 in the adult and aged groups, and found that the increase of DNA synthesis in adult group was more prominent than the aged group at the IGF-1 dose of 5 ($p < 0.005$) and 50 ($p < 0.001$) ng/ml; however, the difference was marginal in cells treated with 500 ng/ml ($p = 0.06$) of IGF-1. These results

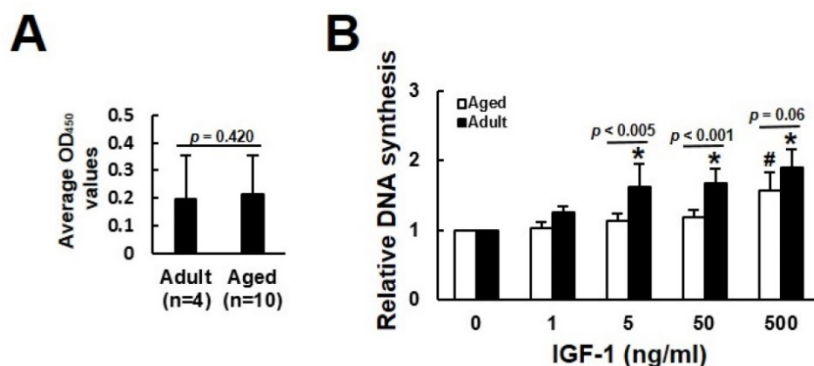


Figure 1. Aging-related changes in the mitogenic response of human bmMSCs to IGF-1. The bmMSCs derived from 4 adult and 10 aged human donors were subjected to BrdU incorporation analyses with or without concomitant treatment of varying doses of IGF-1 as indicated. (A) The average OD₄₅₀ values of adult and aged group cultured without IGF-1 treatment are shown. The difference between the groups was analyzed by the Student's t-test. (B) Relative DNA synthesis in adult and aged cells was calculated by comparing the OD₄₅₀ readings from the IGF-1-treated cells to those of the untreated adult and aged control (to which a value of 1 was assigned), respectively. Data represent the mean \pm S.D. from three experiments. A one-way ANOVA plus Scheffe's post hoc tests were used to analyze the differences among the untreated and IGF-1-treated groups. *, $p < 0.05$ versus untreated adult control. #, $p < 0.05$ versus untreated aged control. Comparison of the fold-change of DNA synthesis between the adult and aged groups was conducted by Student's t-test.

indicated that the mitogenic activity of bmMSCs in response to IGF-1 was impaired in aged humans; however, higher dose of IGF-1 could stimulate DNA synthesis of the aged bmMSCs.

IGF-1 stimulated osteoblastic differentiation of human bmMSCs.

We then examined if IGF-1 treatment affected the osteoblastogenic potential of human bmMSCs. First, we examined the calcium precipitation activities of bmMSC-5 cells, which were isolated from donor 5, at days 19, 23, and 27 post induction. As shown in Fig. 2A, IGF-1 co-treatment seemed to increase calcium precipitation at day 19, which, however, did not reach statistical significance. At days 23, the calcium precipitation activities of cells co-treated with 50, 250, and 500 ng/ml of IGF-1 were approximately 1.7 ($p < 0.05$), 1.6 ($p < 0.05$), and 1.8 ($p < 0.05$) fold of that of the untreated cells at day 19. At day 27, the calcium precipitation activities of cells co-treated with 50, 250, and 500 ng/ml of IGF-1 were approximately 1.7 ($p < 0.05$), 1.9 ($p < 0.05$), and 1.9 ($p < 0.05$) fold of that of the untreated cells at day 19. Subsequently, we treated the bmMSCs of 10 aged donors with 50 and 250 ng/ml of IGF-1 for 21 days, and examined the expression of alkaline phosphatase, collagen I, and osteopontin, which are parameters of osteoblastic differentiation. RT-qPCR analyses showed that their expression levels in cells treated with 250 ng/ml of IGF-1 were approximately 1.8, 2.5, and 1.6 fold of that of untreated cells (Fig. 2B). The donor-specific data were shown in the supplemental Table S2-S4. We also compared the osteoblastic differentiation capability of adult (bmMSC-1, bmMSC-2, bmMSC-3) and aged (bmMSC-5, bmMSC-6, bmMSC-7) cells which were either left untreated or co-treated with 50 and 250

ng/ml of IGF-1 for 11, 19, 23, and 27 days. In the adult group, and compared with the untreated cells at each time point, 50 and 250 ng/ml of IGF-1 caused approximately 79% and 125% ($p < 0.05$) increase in calcium precipitation at day 11; approximately 38% ($p < 0.05$) and 63% ($p < 0.05$) increase at day 19; approximately 96% and 235% ($p < 0.05$) increase at day 23; and approximately 119% and 152% ($p < 0.05$) increase at day 27, respectively (Fig. 2C). It is worthy to note that we observed that osteoblastic induction by itself caused robust calcium precipitation on the untreated cells at days 23 and 27 post-induction, which might mask the enhancing effect of IGF-1 co-treatment. The difference in

the calcium precipitation activity between the untreated aged and adult groups at all-time points did not reach statistical significance (Fig. 2C). In the aged group, and compared with the untreated adult cells at each time point, 50 and 250 ng/ml of IGF-1 caused approximately 41% ($p < 0.05$) and 34% ($p < 0.05$) increase in calcium precipitation at day 11; approximately 23% ($p < 0.05$) and 30% ($p < 0.05$) increase at day 19; and approximately 97% ($p < 0.05$) and 102% ($p < 0.05$) increase at day 27, respectively (Fig. 2C). Although 50 and 250 ng/ml of IGF-1 caused approximately 82% and 83% increase at day 23, the changes did not reach statistical significance due to the variation among the three lines of cells. In comparison, adult cells treated with 50 ng/ml of IGF-1 showed stronger differentiation capability than aged cells at day 19, whereas 250 ng/ml of IGF-1 treatment caused significant difference in the stimulation of differentiation between these two groups of cells at days 11, 19, and 23. At day 27, the difference in differentiation between adult and aged cells treated with 50 and 250 ng/ml of IGF-1 did not reach statistical significance (Fig. 2C). Taken together, our data suggested that the osteoblastic

differentiation of the adult bmMSCs was more responsive to IGF-1, and that exogenous IGF-1 could stimulate the osteoblastic differentiation capability of bmMSCs of the aged donors.

Overexpression of IGF-1 stimulated the proliferation and osteoblastic differentiation of bmMSCs from aged donors.

The findings that exogenous IGF-1 stimulated the DNA synthesis and the osteoblastic differentiation of bmMSCs led us to investigate if increase of IGF-1 production in the bmMSCs of aged donors resulted in the same outcomes. We established IGF-1-overexpressing bmMSC-5-IGF-1 and bmMSC-8-IGF-1 cells. RT-qPCR analyses showed that the IGF-1 mRNA levels in these cells were approximately 50 and 40 fold of that of corresponding controls (Fig. 3A). Because serum contains a lot of growth factors which stimulate cell proliferation, we used serum-reduced medium in the experiment. Cell proliferation analyses showed that bmMSC-5-IGF-1 and bmMSC-8-IGF-1 cells maintained in serum-reduced media were more proliferative than their corresponding controls (Fig. 3B). Our data

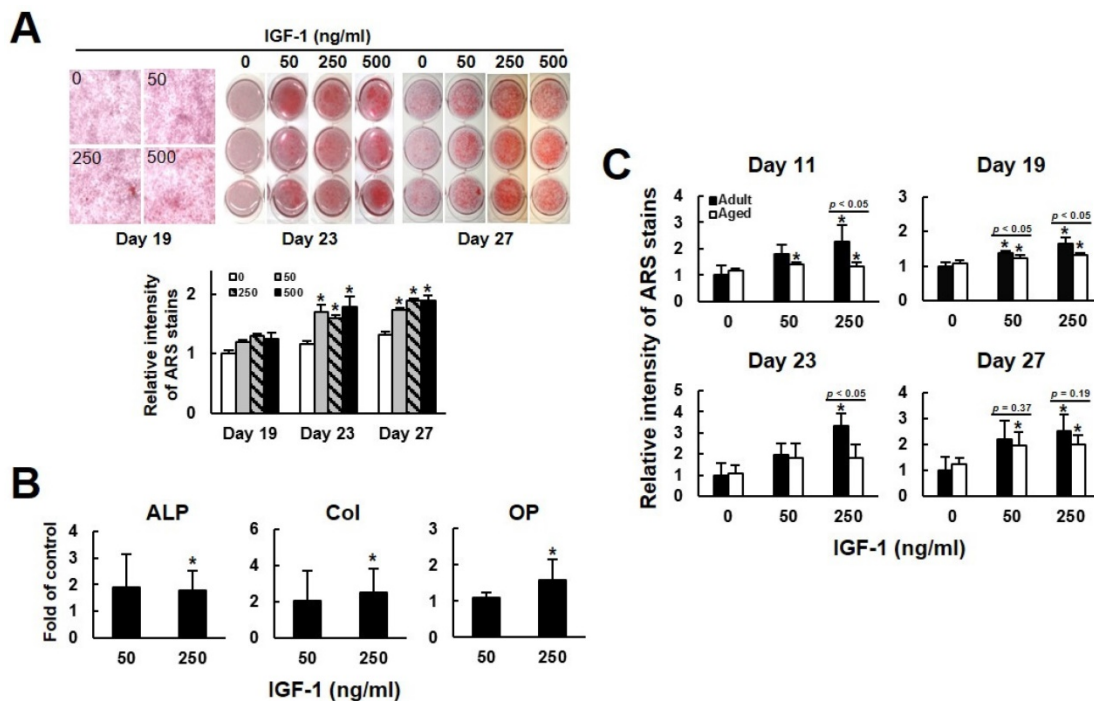


Figure 2. The effects of IGF-1 to the osteoblastic differentiation of human bmMSCs. (A) Osteoblastic differentiation. BmMSC-5 cells were induced to undergo osteoblastic differentiation with or without concomitant treatment of varying doses of IGF-1 as indicated. Cells were stained with Alizarin Red S at the days as indicated. The stains were quantitated. All of the OD₅₉₅ readings of cells were compared to that of the untreated cells of day 19 (to which a value of 1 was assigned). Data represent the mean ± S.D. from three experiments. A one-way ANOVA plus Scheffe's post hoc tests were used to analyze the differences. *, $p < 0.05$ versus the untreated cells of day 19. (B) RT-qPCR analyses. The bmMSCs from 10 aged donors were induced to the osteoblastic lineage without or with concomitant treatment of 50 and 250 ng/ml IGF-1 for 21 days. Cellular levels of alkaline phosphatase (ALP), collagen I (Col), osteopontin (OP), and β-actin mRNAs were measured. Normalized signals from cells treated with IGF-1 were compared to those of cells without IGF-1 treatment (to which a value of 1 was assigned). Data represent the mean ± S.D. from three experiments. *, $p < 0.05$ versus corresponding control. (C) Osteoblastic differentiation. bmMSC-1, -2, and -3 from adult donors and bmMSC-5, -6, and -7 from aged donors were induced to undergo osteoblastic differentiation with or without concomitant treatment of varying doses of IGF-1 as indicated. Cells were stained with Alizarin Red S at the days as indicated. All the OD₅₉₅ readings of cells were compared to that of the untreated adult cells at each time point (to which a value of 1 was assigned). Data represent the mean ± S.D. from three experiments. A one-way ANOVA plus Scheffe's post hoc tests were used to analyze the differences. *, $p < 0.05$ versus untreated adult control. Comparison of the fold-change between the adult and aged groups was conducted by Student's t-test.

showed that serum-reduced medium was not able to stimulate proliferation, which served as a control to manifest the biological effect of IGF-1 overexpression. That the relative cell number in IGF-1 overexpressing cells dropped from day 8 to day 12 indicated that in addition to IGF-1, the other factors provided by higher concentration of serum were required to support long-term proliferation.

To examine the effect of IGF-1 overexpression on the bone-forming capability of aging bmMSCs, a constantly perfused bioreactor was utilized. First, we compared the morphology of the monolayer bmMSC-5 cultures to that of bmMSC-5 cells grown in calcium-alginate scaffolds under static condition. Using light microscope, we found that the monolayer cultures presented spindle shape and the specific characteristic of directional growth (Fig. 4A). In contrast, cells grown in scaffolds were round shape as revealed by SEM (Fig. 4B1-3). The cells could not self-aggregate into clusters after 7 and 14 days (indicated by green arrows) in static cultivation, but could pile up onto the surface of the scaffolds (indicated by blue arrows) after 21 days (Fig. 4B3). Next, we seeded bmMSC-5 and bmMSC-5-IGF-1 cells into calcium-alginate scaffolds separately, and cultured in separate cell culture tanks in the bioreactor for 1, 7, 14, and 21 days. It was noted that bmMSC-5 cells scattered within the scaffolds at day 1, and slowly aggregated into clusters during days 7, 14, and 21 (Figs. 4C1-4), which was different from that of cells cultured under static condition as described in figure 4B1-3. So, constant perfusion appeared to be important for cell-cluster formation. Interestingly, the bmMSC-5-IGF-1 cells had already aggregated into clusters at day 1 (indicated by red arrows) (Fig. 4D1). The clusters seemed to become condensed at day 7 (indicated by yellow arrows), and maintained

condensed stereoscopic during days 14 and 21 (Figs. 4D2-4). On the other hand, we extracted RNAs from the scaffolds of days 7 and 14, and examined the expression of Runx2 (the major regulator of osteoblastic differentiation) and alkaline phosphatase mRNAs. RT-qPCR analyses showed that the expression of these mRNAs in bmMSC-5-IGF-1 cells were approximately 2.4 and 2.9 fold, respectively, of those of bmMSC-5 cells at day 7, and that the Runx2 mRNA level of bmMSC-5-IGF-1 cells was approximately 3.8 fold of that of bmMSC-5 cells at day 14 post osteoblastic induction (Fig. 5). Taken together, these data suggested that IGF-1 overexpression was able to enhance the osteogenic potential of bmMSC-5 cells, and might improve the capability of bmMSC-5 cells to aggregate to produce bone-like tissues.

Live/Dead staining of bmMSC clusters in calcium-alginate scaffolds.

We then evaluated the viability of bmMSCs in the clusters inside the scaffolds using two-color fluorescent staining, calcein AM and propidium iodide (PI). Results showed that the percentage of dead cells in the clusters of bmMSC-5 cells was approximately 1.4%, 44.5%, 55.6%, and 39.8% as measured at days 1, 7, 14, and 21, respectively; and the cell death was concentrated at the center of the clusters (Fig. 6, A1-D3). In sharp contrast, the percentage of dead cells in the clusters of bmMSC-5-IGF-1 cells was approximately 0.1%, 10.8%, 8.8%, and 6.4% as measured at days 1, 7, 14, and 21, respectively (Fig. 6, E1-H3). These data suggested that while medium perfusion could support cells to aggregate into clusters in scaffolds, IGF-1 could improve the survival rate of bmMSCs in the clusters during osteogenesis in the bioreactor system.

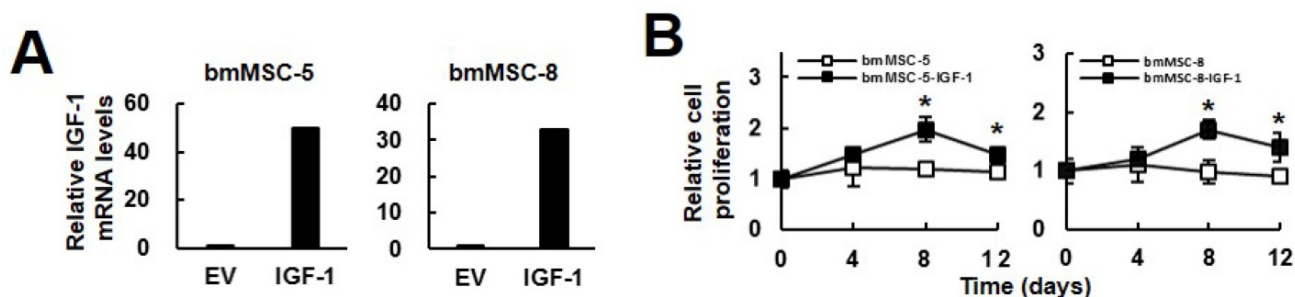


Figure 3. Effect of IGF-1 overexpression on the proliferation and osteoblastic differentiation of aging bmMSCs. (A) RT-qPCR analyses. BmMSC-5 and bmMSC-8 cells were infected with Lenti virus for IGF-1 overexpression. The expression of IGF-1 mRNA in bmMSC-5, bmMSC-5-IGF-1, bmMSC-8, and bmMSC-8-IGF-1 cells was measured. (B) Cell proliferation assays. BmMSC-5, bmMSC-5-IGF-1, bmMSC-8, bmMSC-8-IGF-1 cells were cultured in media containing 2.5% of serum. Cells were harvested and counted at the time indicated. Relative cell proliferation was calculated by comparing the cell number at days 4, 8, and 12 to that of day 0 (to which a value of one was assigned). Data represent the mean \pm S.D. from three experiments. *, $p < 0.01$ versus corresponding control.

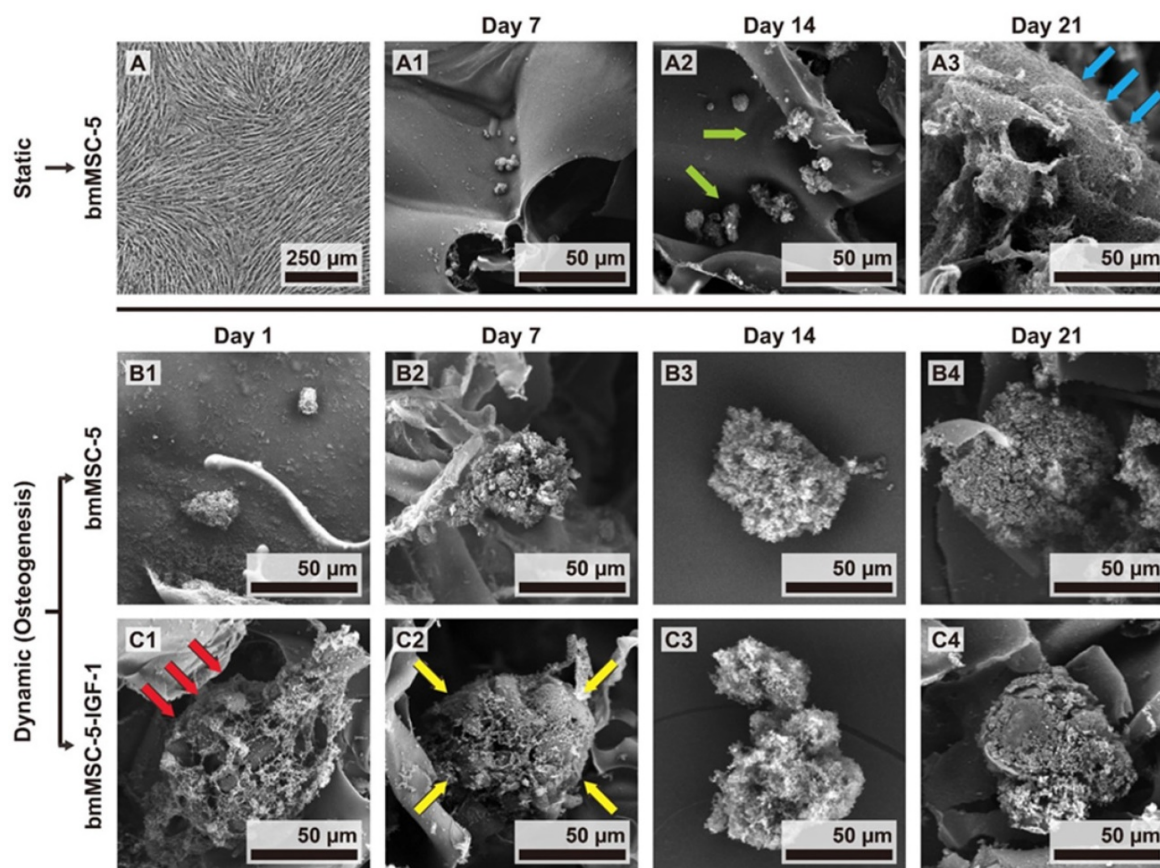


Figure 4. The morphology of bmMSC-5 cells under static and dynamic culture conditions. (A) The morphology of bmMSC-5 cells in 2-dimensional culture plates in static culture condition was examined by light microscopy. Representative photo is shown. (B) The morphology of bmMSC-5 cells in calcium-alginate scaffolds incubated in 2-dimensional culture plates in static culture condition for 7, 14, and 21 days were examined by SEM. Representative photos are shown. (C, D) bmMSC-5 and bmMSC-5-IGF-1 cells were seeded into calcium-alginate scaffolds and kept in static state to stabilize cells in 3-dimensional environment for 24 h, and then transferred to dynamic perfused bioreactor. The morphology of bmMSC-5 and bmMSC-5-IGF-1 cell clusters in scaffolds incubated in bioreactor for 1, 7, 14, and 21 days was examined by SEM. Representative photos are shown.

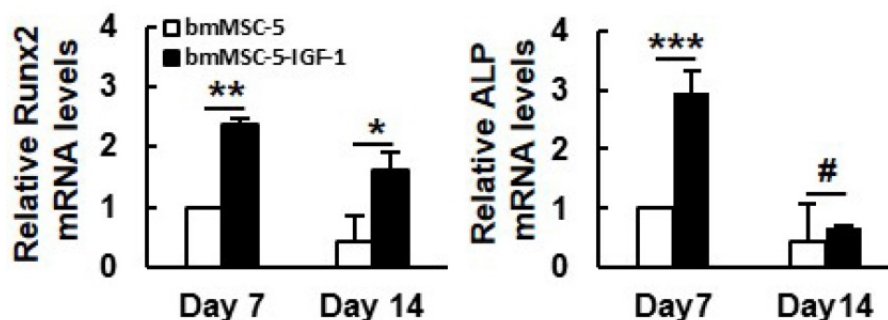


Figure 5. Effect of IGF-1 overexpression to the osteoblastic differentiation of 3-dimensional bmMSC-5 cultures. Scaffolds which contained either bmMSC-5 or bmMSC-5-IGF-1 cells, and were incubated under osteoblastic induction in bioreactor were collected at days 7 and 14 for total RNA preparation. The levels of Runx2, alkaline phosphatase (ALP) and β -actin mRNAs were measured by RT-qPCR analyses. Normalized signals were compared to those of bmMSC-5 cells of day 7 (to which a value of one was assigned). Data represent the mean \pm S.D. from three experiments. *, $p < 0.05$; **, $p < 0.005$; ***, $p < 0.001$; #, $p = 0.585$ versus corresponding bmMSC-5 control.

Size distribution and biomineralization of bmMSC clusters.

Next, we analyzed the size distribution of the cell clusters using SEM (Supplemental Fig. S3), and calculated data in Supplemental Fig. S4. At day 1, there was no bmMSC-5 cell clusters found in the scaffolds; whereas approximately 91.9% of

bmMSC-5-IGF-1 cells formed clusters with size bigger than 100 μm (Fig. 7A1). At day 7, approximately 52.9% and 5.9% of bmMSC-5 cells formed clusters with sizes around 50-100 μm and 100-150 μm , respectively; whereas approximately 53.8%, 15.4%, and 30.8% of bmMSC-5-IGF-1 cells formed clusters with sizes around 50-100 μm , 100-150 μm , and bigger than 150 μm , respectively (Fig. 7A2). At day 14,

approximately 50%, 12.5%, and 25% of bmMSC-5 cells, and approximately 22.2%, 11.1%, and 66.7% of bmMSC-5-IGF-1 cells formed clusters with sizes around 50-100 μm , 100-150 μm , and bigger than 150 μm , respectively (Fig. 7A3). At day 21, approximately 37.5%, 25%, and 37.5% of bmMSC-5 cells, and approximately 25%, 33.3%, and 41.7% of bmMSC-5-IGF-1 cells formed clusters with sizes around 50-100 μm , 100-150 μm , and bigger than 150 μm , respectively (Fig. 7A4). These data showed that bmMSC-5 cells were able to form clusters with increasing sizes with time, but IGF-1 overexpression seemed to facilitate the rate of cluster formation. Also, we estimated cell numbers per cluster via F-actin staining (Supplemental Fig. S5). Briefly, we identified the volume of cell clusters by F-actin staining, and calculated the cell numbers with Hoechst 33342 staining for both conditions with every time points. Then we got the relative cell volume (Fig. 7D) and cell numbers in different size of bone-like tissues during the cell cultivation (Fig. 7E) using Imaris Scientific 3D/4D Image Processing & Analysis Software (Bitplane, CT, USA). Moreover, the histological staining revealed that most bone-like tissues exhibited a round or elliptical shape (Supplemental Fig. S6).

In parallel, we analyzed the biomineralization status of the cell clusters. Biomineralization takes place during the final stage of bone formation. We stained the cell clusters collected at days 1, 7, 14, and 21 with xylene orange, a fluorochrome widely used for labeling calcified tissues. The results showed that the calcified areas of both bmMSC-5 and bmMSC-5-IGF-1 cell clusters increased with time,

indicating the occurrence of biomineralization in these cell clusters. Notably, the biomineralization status of bmMSC-5-IGF-1 cell clusters was more prominent, examined at all-time points, than that of bmMSC-5 cell clusters (Fig. 7, B and C). These data indicated that IGF-1 overexpression promoted bmMSCs to form bone-like tissues.

XRD and FT-IR determination of bone-like tissues.

To examine if the differentiated bmMSC-5 and bmMSC-5-IGF-1 cells secreted biological apatite, we collected the precipitates from the media in the bottles containing either bmMSC-5 scaffolds or bmMSC-5-IGF-1 scaffolds at day 21, and analyzed the X-ray diffraction pattern of these precipitates, with hydroxyapatite as a standard. As shown in both groups of precipitates, there were specific peaks at (002) plane and (211) plane, a pattern matching to the diffraction pattern of hydroxyapatite (Fig. 8A). We also analyzed the precipitates using FT-IR spectroscopy. As shown in figure 8B, the most impressive peaks which lay at 1200-900 and 600-500 cm^{-1} were attributed to phosphate groups. The peaks displayed between 1650 and 1300 cm^{-1} were attributed to carbonate groups. A broad hydroxyl bending mode was exhibited around 3500-3100 cm^{-1} . Taken together, these data showed that both bmMSC-5 and bmMSC-5-IGF-1 cells produced biological apatite in the bioreactor under osteogenic induction, and suggested that the bone-like tissues cultured in the bioreactor were moving toward to mature bones.

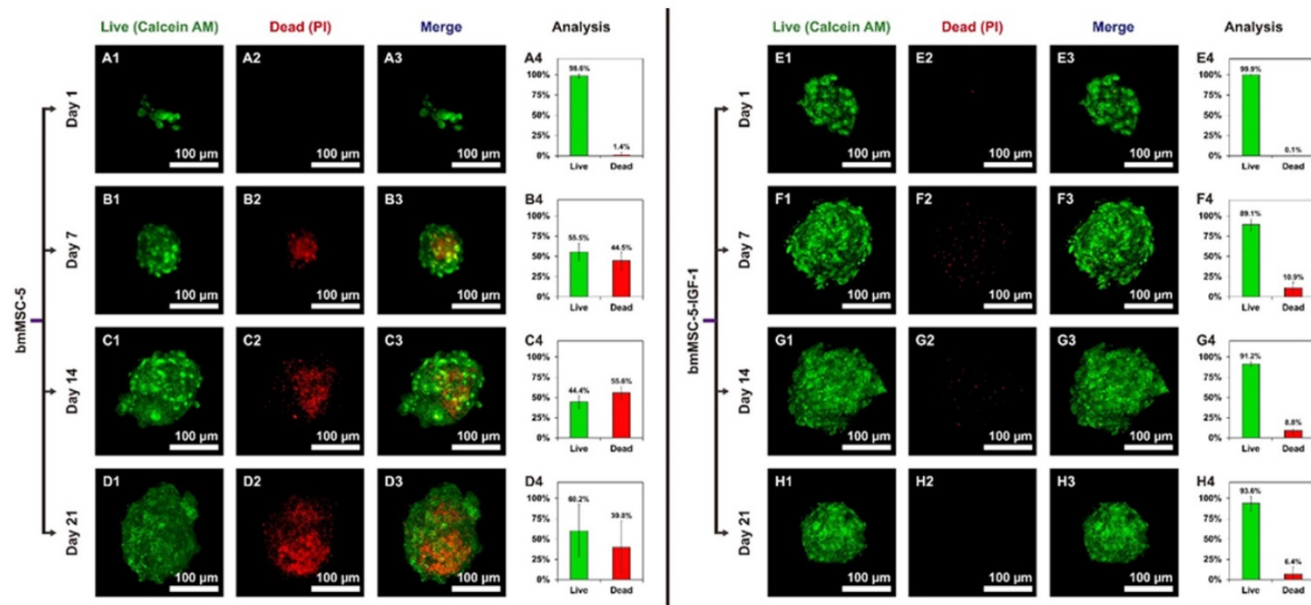


Figure 6. Live/Dead staining of bmMSC cell clusters in calcium-alginate scaffolds. The scaffolds seeded with bmMSC-5 or bmMSC-5-IGF-1 cells were retrieved from bioreactor at the time indicated, and stained with calcein AM (A1, B1, C1, D1, E1, F1, G1, and H1) or with PI (A2, B2, C2, D2, E2, F2, G2, and H2). The merged images (A3, B3, C3, D3, E3, F3, G3, and H3) and the calculated percentage of live and dead cells (A4, B4, C4, D4, E4, F4, G4, and H4) were shown.

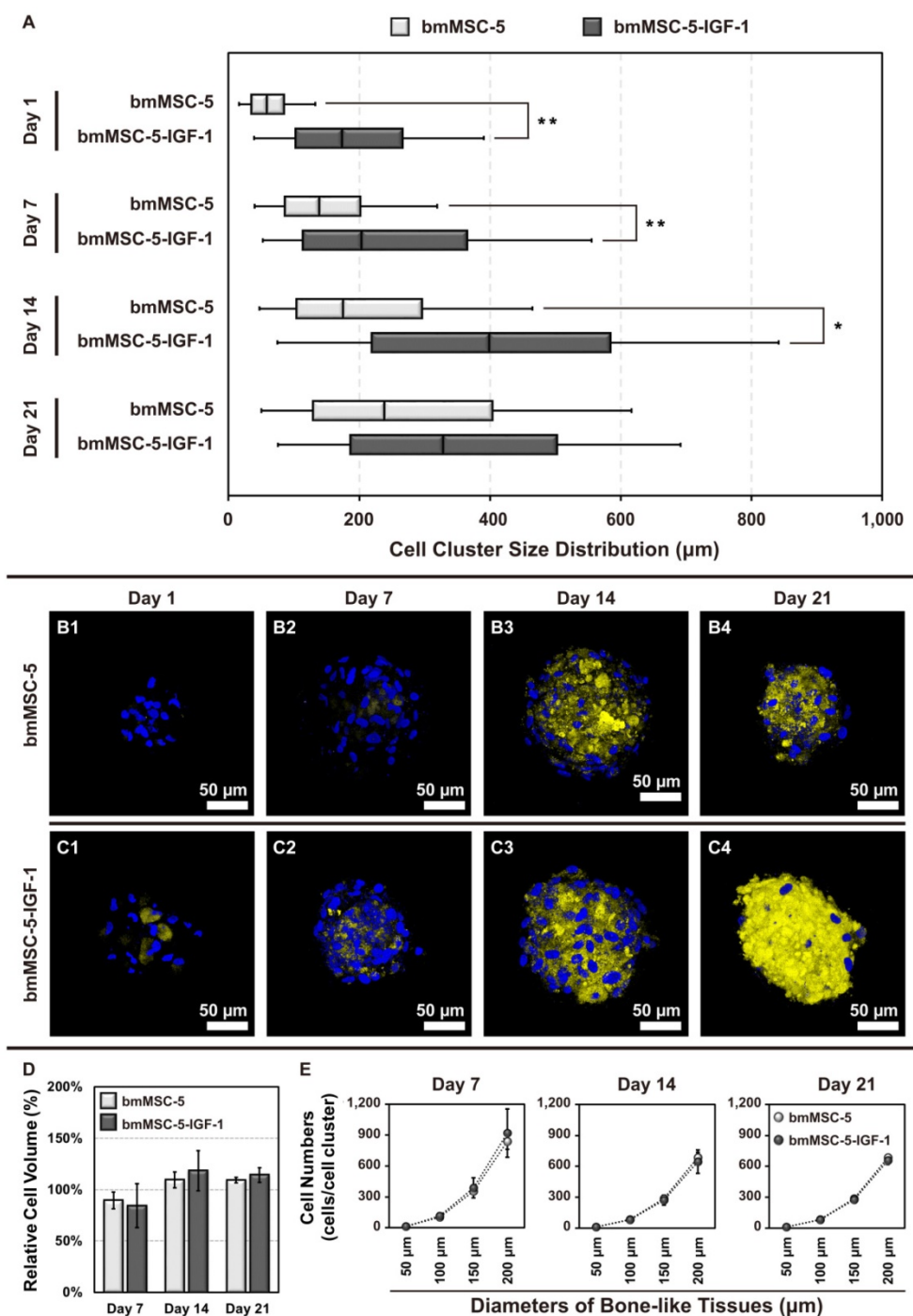


Figure 7. Size distribution, biomineralization and cell numbers of bmMSC cell clusters. (A) The sizes of cell clusters in the scaffolds incubated in bioreactor for 1, 7, 14, and 21 days were measured by SEM (n = 20-35 for each condition, the details were revealed in supplementary Fig. S4). (B, C) The cell clusters were stained with xylenol orange to indicate the biomineralized areas, and with Hoechst 33342 to indicate the location of nucleus. (D) The relative cell volume of bone-like tissues after 7, 14, and 21 days' cultivation were analyzed via F-actin Staining and calculated by Imaris software (normalized with Day 1); and (E) represented cell numbers in different size of bone-like tissues at every time points (the details were revealed in supplementary Table S6). The values of cell cluster size distribution were mean ± S.D.; *p < 0.05, **p < 0.01.

Discussion

BmMSCs are known to be important in the maintenance of fully grown skeleton and in the repair of damaged bones, but how bmMSCs lose osteoblastogenic potential with aging has not been fully elucidated. Thus, understanding of the

underlying mechanisms may help to developing effective strategies not only to boost bone formation in the elderly, but also to improve the osteogenic performance of aging bmMSCs for possible application of autologous bmMSCs to repair bone defect of the elderly.

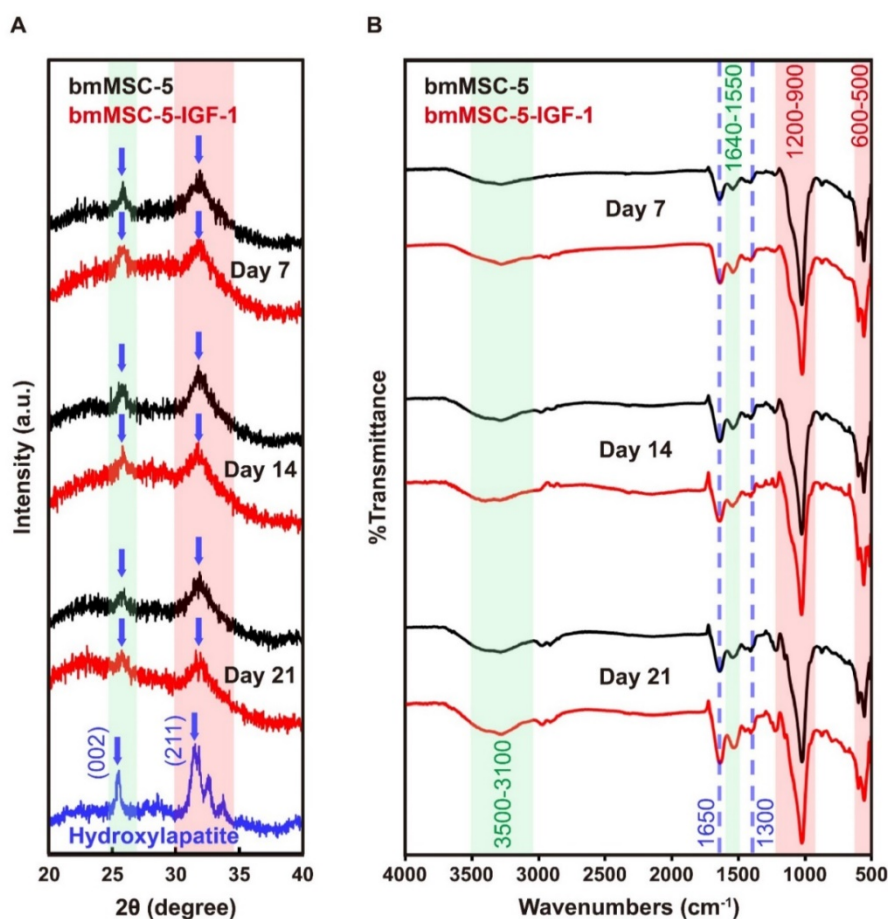


Figure 8. Characterization of the biological apatite secreted by bmMSC-5 and bmMSC-5-IGF-1 cells in the bioreactor. After 21 days of incubation, the scaffolds were removed, and the media were centrifuged to collect the precipitates. The precipitates were dried and subjected to XRD examination using hydroxylapatite as a standard (A). The precipitates were also analyzed using FT-IR for the presence of phosphate, carbonate, and hydroxyl groups (B).

Our data point out that the mitogenic activity of human bmMSCs in response to IGF-1 is impaired with aging, and that the effect of aging on the mitogenic activity of human bmMSCs without IGF-1 supplement is not significant (Fig. 1). These phenomena are consistent with that noted in murine system [24]. However, our data further indicated that defect in IGF-1 signaling could be one of the major causes in aging-related loss of osteoblastogenic potential in human bmMSCs. Evidences supporting this notion came from the findings that (i) while PDGF and FGF inhibited differentiation of rat bmMSCs [20, 22], IGF-1 was able to promote osteoblastic differentiation of rat [24] and human bmMSCs, and (ii) under osteoblastic induction, aging human bmMSCs showed lessened and delayed calcium precipitation in response to IGF-1 treatment, compared to cells from adult donor (Fig. 2). The mechanisms underlying the aging-related defect in IGF-1 signaling are currently unclear. By examining the expression of IGF-1 receptor (IGF-1R) and its binding to IGF-1R in bmMSCs of adult and aged rats, Tanaka and Liang reported that there were no

significant aging-related differences in these activities, and concluded that the aging-related defect in IGF-1 signaling might occur after the activation of IGF-1Rs [24]. Whether these phenomena also exist in human bmMSCs requires further investigation. In this study, we examined the expression levels of IGF-1 and IGF-1R mRNAs in bmMSCs from 4 adults and 10 aged donors (Table 1) and found that aging seemed not to decrease IGF-1 and IGF-1R expression in human bmMSCs (Supplemental Fig. S1).

Moreover, our previous studies have suggested that alterations in glycosylation patterns of bmMSCs might play an important role in the aging of human bmMSC [34]. IGF-1R contains several N-glycans [35, 36], and it has been shown that inhibition of N-glycosylation altered cell surface abundance of IGF-1R and blocked IGF action [36, 37]. Therefore, it is tempting to speculate that the glycosylation status of IGF-1R on human bmMSCs might be altered with aging, causing the defect of IGF-1 signaling in bmMSCs of the elderly, or alternatively, but not mutual exclusively, that the aging-related changes in the composition of membrane glycoproteins of

bmMSCs might be a contributor to the decreased response to IGF-1. Indeed, we found that the expression of decorin (DCN), a proteoglycan, was up-regulated with aging in human and rat bmMSCs, and that DCN knockdown increased the mitogenic activity of aging human bmMSCs in response to IGF-1 (unpublished data). Given the finding that DCN could bind to IGF-1R in renal fibroblasts [38], it is possible that exogenous IGF-1 might compete with DCN for binding to and activate IGF-1R of bmMSCs, which promoted the proliferation and osteogenic potential of aging human bmMSCs.

Our data showed that without IGF-1 co-treatment, the osteoblastic differentiation activity of bmMSCs from aged donors was similar to that of bmMSCs from adult donors (Fig. 2C). To interpret this set of data, it is worthy to note that by examining the ectopic bone formation of untreated and dexamethasone-treated bmMSCs (isolated from adult and aged rats) which were implanted into adult and aged rats, Quarto et al. reported that untreated bmMSCs from aged rats were defective in bone induction potential and the environment in aged recipients did not support bone formation; however, there were no appreciable difference in the bone-forming capability between the dexamethasone-treated adult and aging bmMSCs [10]. Therefore, in our study, dexamethasone might fully activate the osteogenic potential and abolish the age difference in cells without IGF-1 treatment. With this in mind, our data manifest the aging-related impairment in osteogenic potential in the way that the induction of osteoblastic differentiation in aging bmMSCs were less responsive to IGF-1 than that in adult bmMSCs.

Based on our data, it seems to be reasonable to use exogenous IGF-1 to activate bmMSCs *in vivo* to intervene the loss of bone mass in the elderly. However, systemic IGF-1 application increases the risk of tumorigenesis, too [39]. We thought that it would be more practical by delivering the activated autologous bmMSCs *in situ* to repair local bone damage in the elderly. For this purpose, the activated aging bmMSCs must exhibit improved response to osteogenic-inducing signals and their subsequent bone-forming capability. The bioreactor system allowed us to grow bmMSCs in 3-dimensional environment with constant medium flow which mimics the *in vivo* microenvironment, and to provide cells osteogenic-inducing signals [32]. Such an experimental setting enabled us to address the effect of IGF-1 to the bone-forming capability of aging bmMSCs. By analyzing the formation, size distribution, and the biomineralization status of cell clusters, and the cell death in the clusters, and by

characterizing the secreted biological apatite, we found that IGF-1 overexpression could enhance the bone-forming capability of aging bmMSCs. Thus, our data indicate that IGF-1 overexpression is an effective strategy in activating aging autologous bmMSCs *in vitro* for limited *in situ* delivery to repair local bone damage in the elderly.

The mechanism as to how IGF-1 overexpression enhanced the bone-forming capability of aging bmMSCs was not extensively investigated in this study. Based on our data that IGF-1 overexpression increased cell proliferation (Fig. 3), and increased the expression of Runx2 in the 3-dimensional cultures (Fig. 5), it is tempting to speculate that IGF-1 overexpression might increase IGF-1 signaling, leading to enhanced osteoblastic differentiation of bmMSCs. Indeed, it has been well documented that IGF-1 functions not only as a progression factor, but also as an enhancer of glucose uptake and an inhibitor of cell death [42, 43]. Thus, in our study as described in Fig. 6, IGF-1 overexpression might elicit these effects to help the cells which were located in the center of the cell clusters survive, proliferate, and differentiate in the relatively hypoxic and mal-nutritional environment, hence an improved survival rate and bone-forming capability. Whether IGF-1 overexpression activated the IGF-1R of aging bmMSCs by competing with DCN for IGF-1R-binding is currently under investigation.

It is worthy to note that while we incubated the calcium-alginate scaffolds seeded with either bmMSC-5 or bmMSC-5-IGF-1 cells in culture dishes containing media absent of osteogenic supplements, bmMSC-5-IGF-1 but not bmMSC-5 cells formed clusters in 24 h (data not shown). Given the fact that bmMSC-5 cells under osteogenic induction also gradually formed clusters in the bioreactor, modulation of cell-cell interaction might be important for IGF-1 to promote osteoblastic differentiation of aging bmMSCs. Moreover, it took much less time for bmMSC-5-IGF-1 cells cultured in scaffolds to show the morphological effect of IGF-1 (Fig. 4) compared with that of bmMSC-5 cells cultured in 2-dimensional dishes in the presence of IGF-1 (Fig. 2). Therefore, it would be more informative to study the biological effect of IGF-1 on bmMSCs using 3-dimensional cultures.

An alternative way to apply the IGF-1 overexpressing aging bmMSCs in treating bone defects is to use these cells to produce bone graft materials. Bone graft materials are often required for the treatment of large bone defects [40, 41]. Producing appropriate bioactive bone graft materials for bone regeneration is a crucial issue in orthopedics. The bioreactor system used in this study was designed for

this purpose [32, 33]. This system provides constant medium flow to replenish the nutrition supply in scaffolds to maintain cell survival in the scaffolds for achieving tissue uniformity throughout the bone-like tissues. Even so, our data showed that the death of bmMSC-5 cells still increased with time in the inner region of scaffolds (Fig. 6, A1-D3). However, the death of bmMSC-5-IGF-1 cells under the same experiment setting was almost neglectable (Fig. 6, E1-H3). So, the IGF-1 produced by bmMSC-5-IGF-1 cells was able to maintain cell survival, and result in more uniform mineralization (Fig. 7, B and C). Our data support the introducing of IGF-1 into autologous aging bmMSCs to improve the production of bone graft materials in bioreactors.

Conclusion

In this study, we showed that the IGF-1 signaling of human bmMSCs is impaired in aging, which compromises the osteogenic capability of the aging bmMSCs. We also showed that transduction of an osteoinductive growth factor gene, IGF-1, into the aging bmMSCs can enhance their osteogenic capability. Our studies, on one hand, pointed out possible applications of autologous bmMSCs in the repair of bone defect in the elderly. On the other hand, our data suggested that further elucidation of the mechanisms underlying the impaired response of aging bmMSCs to IGF-1 may provide us clues for developing strategies to sensitize the aging bmMSCs to the physiological levels of IGF-1, which may improve bone formation activity in the elderly.

Supplementary Material

Supplementary figures and tables.
<http://www.thno.org/v07p1598s1.pdf>

Acknowledgements

We would like to thank Dr. Shau-Ku Huang for the critical reading of this manuscript, and the staff of the First Core Lab (Collage of Medicine, NTU) for technical support and helpful discussions. The use of human bmMSCs in this study was approved by the Internal Ethical Committee of National Health Research Institutes, Taiwan (IRB No. EC0970204). Yen-Liang Lai carried out his thesis research under the auspices of the Ph.D. Program in Tissue Engineering and Regenerative Medicine, National Chung Hsing University and National Health Research Institutes.

Competing Interests

The authors have declared that no competing interest exists.

References

- Zaidi M. Skeletal remodeling in health and disease. *Nat Med.* 2007; 13: 791-801.
- Baron R, Kneissel M. WNT signaling in bone homeostasis and disease: from human mutations to treatments. *Nat Med.* 2013; 19: 179-92.
- Yang KC, Wang CC, Wu CC, Hung TY, Chang HC, Chang HK, et al. Acute and subacute oral toxicity tests of sintered dicalcium pyrophosphate on ovariectomized rats for osteoporosis treatment. *Biomed Eng-App Bas C.* 2010; 22: 169-76.
- Guan M, Yao W, Liu R, Lam KS, Nolte J, Jia J, et al. Directing mesenchymal stem cells to bone to augment bone formation and increase bone mass. *Nat Med.* 2012; 18: 456-62.
- Verma S, Rajaratnam J, Denton J, Hoyland J, Byers R. Adipocytic proportion of bone marrow is inversely related to bone formation in osteoporosis. *J Clin Pathol.* 2002; 55: 693-8.
- Rosen CJ, Bouxsein ML. Mechanisms of disease: is osteoporosis the obesity of bone? *Nat Rev Rheumatol.* 2006; 2: 35-43.
- Duque G, Rivas D, Li W, Li A, Henderson JE, Ferland G, et al. Age-related bone loss in the LOU/c rat model of healthy ageing. *Exp Gerontol.* 2009; 44: 183-9.
- Tonna EA. Electron microscopic study of bone surface changes during aging. The loss of cellular control and biofeedback. *J Gerontol.* 1978; 33: 163-77.
- Tsuji T, Hughe F, McCulloch C, Melcher A. Effects of donor age on osteogenic cells of rat bone marrow in vitro. *Mech Ageing Dev.* 1990; 51: 121-32.
- Quarto R, Thomas D, Liang C. Bone progenitor cell deficits and the age-associated decline in bone repair capacity. *Calcif Tissue Int.* 1995; 56: 123-9.
- Owen M, Friedenstein A. Stromal stem cells: marrow-derived osteogenic precursors. *Ciba Found Symp.* 1988; 136: 42-60.
- Bruder SP, Fink DJ, Caplan AI. Mesenchymal stem cells in bone development, bone repair, and skeletal regeneration therapy. *J Cell Biochem.* 1994; 56: 283-94.
- Prockop DJ. Marrow stromal cells as stem cells for nonhematopoietic tissues. *Science.* 1997; 276: 71-4.
- Pittenger MF, Mackay AM, Beck SC, Jaiswal RK, Douglas R, Mosca JD, et al. Multilineage potential of adult human mesenchymal stem cells. *Science.* 1999; 284: 143-7.
- Halleux C, Sottile V, Gasser J, Seuwen K. Multi-lineage potential of human mesenchymal stem cells following clonal expansion. *J Musculoskelet Neuronal Interact.* 2001; 2: 71-6.
- Shuai Y, Liao L, Su X, Yu Y, Shao B, Jing H, et al. Melatonin Treatment Improves Mesenchymal Stem Cells Therapy by Preserving Stemness during Long-term In Vitro Expansion. *Theranostics.* 2016; 6: 1899.
- Liang C, Barnes J, Seedor J, Quartuccio H, Bolander M, Jeffrey J, et al. Impaired bone activity in aged rats: alterations at the cellular and molecular levels. *Bone.* 1992; 13: 435-41.
- Singh L, Brennan TA, Russell E, Kim J-H, Chen Q, Johnson FB, et al. Aging alters bone-fat reciprocity by shifting in vivo mesenchymal precursor cell fate towards an adipogenic lineage. *Bone.* 2016; 85: 29-36.
- Moerman EJ, Teng K, Lipschitz DA, Lecka-Czernik B. Aging activates adipogenic and suppresses osteogenic programs in mesenchymal marrow stroma/stem cells: the role of PPAR- γ 2 transcription factor and TGF- β /BMP signaling pathways. *Aging Cell.* 2004; 3: 379-89.
- Tanaka H, Liang CT. Effect of platelet-derived growth factor on DNA synthesis and gene expression in bone marrow stromal cells derived from adult and old rats. *J Cell Physiol.* 1995; 164: 367-75.
- Nazari M, Ni NC, Lüdke A, Li S-H, Guo J, Weisel RD, et al. Mast cells promote proliferation and migration and inhibit differentiation of mesenchymal stem cells through PDGF. *J Mol Cell Cardiol.* 2016; 94: 32-42.
- Tanaka H, Ogasa H, Barnes J, Liang CT. Actions of bFGF on mitogenic activity and lineage expression in rat osteoprogenitor cells: effect of age. *Mol Cell Endocrinol.* 1999; 150: 1-10.
- Colenci R, da Silva Assunção LR, Bomfim SRM, de Assis Golim M, Deffune E, Oliveira SHP. Bone marrow mesenchymal stem cells stimulated by bFGF up-regulated protein expression in comparison with periodontal fibroblasts in vitro. *Arch Oral Biol.* 2014; 59: 268-76.
- Tanaka H, Liang CT. Mitogenic activity but not phenotype expression of rat osteoprogenitor cells in response to IGF-I is impaired in aged rats. *Mech Ageing Dev.* 1996; 92: 1-10.
- Huat TJ, Khan AA, Pati S, Mustafa Z, Abdullah JM, Jaafar H. IGF-1 enhances cell proliferation and survival during early differentiation of mesenchymal stem cells to neural progenitor-like cells. *BMC Neurosci.* 2014; 15: 1.
- Li WT, Hu WK, Ho FM. High glucose induced bone loss via attenuating the proliferation and osteoblastogenesis and enhancing adipogenesis of bone marrow mesenchymal stem cells. *Biomed Eng-App Bas C.* 2013; 25: 1340010.
- Xian L, Wu X, Pang L, Lou M, Rosen CJ, Qiu T, et al. Matrix IGF-1 maintains bone mass by activation of mTOR in mesenchymal stem cells. *Nat Med.* 2012; 18: 1095-101.
- Benedict MR, Adiyaman S, Ayers DC, Thomas FD, Calore JD, Dhar V, et al. Dissociation of bone mineral density from age-related decreases in insulin-like growth factor-I and its binding proteins in the male rat. *J Gerontol.* 1994; 49: B224-B30.

29. Tanaka H, Barnes J, Liang C. Effect of age on the expression of insulin-like growth factor-I, interleukin-6, and transforming growth factor- β mRNAs in rat femurs following marrow ablation. *Bone*. 1996; 18: 473-8.
30. Waseem M, Khan I, Iqbal Ha, Eijaz S, Usman S, Ahmed N, et al. Hypoxic Preconditioning Improves the Therapeutic Potential of Aging Bone Marrow Mesenchymal Stem Cells in Streptozotocin-Induced Type-1 Diabetic Mice. *Cell Reprogram*. 2016; 18: 344-55.
31. Wakisaka A, Tanaka H, Barnes J, Liang CT. Effect of Locally Infused IGF-I on Femoral Gene Expression and Bone Turnover Activity in Old Rats. *J Bone Miner Res*. 1998; 13: 13-9.
32. Chen CY, Ke CJ, Yen KC, Hsieh HC, Sun JS, Lin FH. 3D porous calcium-alginate scaffolds cell culture system improved human osteoblast cell clusters for cell therapy. *Theranostics*. 2015; 5: 643.
33. Chen CY, Chiang TS, Chiou LL, Lee HS, Lin FH. 3D cell clusters combined with a bioreactor system to enhance the drug metabolism activities of C3A hepatoma cell lines. *J Mater Chem B*. 2016; 43: 7000-7008.
34. Jiang SS, Chen C-H, Tseng K-Y, Tsai F-Y, Wang MJ, Chang I-S, et al. Gene expression profiling suggests a pathological role of human bone marrow-derived mesenchymal stem cells in aging-related skeletal diseases. *Aging*. 2011; 3: 672-84.
35. Siddals KW, Marshman E, Westwood M, Gibson JM. Abrogation of insulin-like growth factor-I (IGF-I) and insulin action by mevalonic acid depletion: synergy between protein prenylation and receptor glycosylation pathways. *J Biol Chem*. 2004; 279: 38353-9.
36. Siddals KW, Allen J, Sinha S, Canfield AE, Kalra PA, Gibson JM. Apposite insulin-like growth factor (IGF) receptor glycosylation is critical to the maintenance of vascular smooth muscle phenotype in the presence of factors promoting osteogenic differentiation and mineralization. *J Biol Chem*. 2011; 286: 16623-30.
37. Contessa JN, Bhojani MS, Freeze HH, Rehemtulla A, Lawrence TS. Inhibition of N-linked glycosylation disrupts receptor tyrosine kinase signaling in tumor cells. *Cancer Res*. 2008; 68: 3803-9.
38. Schaefer L, Tsalastra W, Babelova A, Baliova M, Minnerup J, Sorokin L, Grone HJ, Reinhardt DP, Pfeilschifter J, Iozzo RV, Schaefer RM. Decorin-mediated regulation of fibrillin-1 in the kidney involves the insulin-like growth factor-1 receptor and mammalian target of rapamycin. *Am. J. Pathol*. 2007; 170:301-315.
39. Renehan AG, Zwahlen M, Minder C, T O'Dwyer S, Shalet SM, Egger M. Insulin-like growth factor (IGF)-I, IGF binding protein-3, and cancer risk: systematic review and meta-regression analysis. *The Lancet*. 2004; 363:1346-1353.
40. Sun JS, Chen PY, Tsuang YH, Chen MH, Chen PQ. Vitamin-D Binding Protein Does Not Enhance Healing in Rat Bone Defects: A Pilot Study. *Clin Orthop Relat Res*. 2009; 467:3156-3164.
41. Huey DJ, Hu JC, Athanasiou KA. Unlike Bone, Cartilage Regeneration Remains Elusive. *Science*. 2012; 338:917-921.
42. Rajpathak SN, Gunter MJ, Wylie-Rosett J, Ho GYF, Kaplan RC, Muzumdar R, Rohan TE, Strickler HD. The role of insulin-like growth factor-I and its binding proteins in glucose homeostasis and type 2 diabetes. *Diabetes Metab Res Rev*. 2009; 25:3-12.
43. Kooijman R. Regulation of apoptosis by insulin-like growth factor (IGF)-I. *Cytokine Growth Factor Rev*. 2006; 17:305-323.